Proceedings of the 3rd International Seminar of Basic Sciences
©2017 FMIPA Pattimura University, Ambon, Indonesia
ISBN: 978-602-61644-0-7
pp. 11 – 24

FABRICATION AND ELECTROCHEMICAL EVALUATION OF THE LITHIUM BATTERY, $Li_{0.5}La_{0.5}TiO_3$/$LiFePO_4$-C INTERFACE

K. P. Abhilash[1], P.Christopher Selvin[2], B. Nalini[3], M.V. Reddy[1,4,*]

[1]Department of Physics, National University of Singapore, 117542, Singapore
[2]Department of Physics, Bharathiar University, Coimbatore, 642046, India
[3]Department of Physics, Avinashilingam University for Women, Coimbatore, 642043, India
[4]Department of Materials Science and Engineering, National University of Singapore, Singapore, 117576, Singapore

*****_Corresponding author_: phymvvr@nus.edu.sg

ABSTRACT

The $Li_{0.5}La_{0.5}TiO_3$ and $LiFePO_4$/C has been prepared using sol-gel method for its interface analysis towards its application for all solid state assembly. The $LiFePO_4$cathode material and $Li_{0.5}La_{0.5}TiO_3$ solid electrolyte has been individually tested for its electrochemical reversibility. The thin film battery assembly shows severe capacity fading, which results in electrochemically non active with the chosen anode materials. In order to verify the electrochemical activity and interaction of $Li_{0.5}La_{0.5}TiO_3$-$LiFePO_4$/C interface the mixture has been tested for its electrochemical reversibility. The $Li_{0.5}La_{0.5}TiO_3$-$LiFePO_4$/C interface exhibits well resolved oxidation-reduction hype which verifies its suitability towards all solid state assemblies.

Keywords: *Electrochemical reversibility; Interface, Oxidation-reduction; Solid state thin film assembly*

1. INTRODUCTION

In recent times, efforts have been devoted to energy based research due to their increasing demand, raise in oil prices, uncertainty in energy supplies, etc. Electrical energy is the most versatile form of energy available to the human beings simply for the reasons that it can be transported easily and reconverted into other forms. Increased use of renewable energy is recognized to be both economically as well as environmentally sound alternative. This in turn increases the demand for the development of storage systems such as Lithium ion batteries. Requirement for improving the battery properties

includes, cycleability, reversibility, high energy, power density, safety, environmental impact, lower cost, etc. Hence, a wide range of materials (anodes, cathodes and electrolytes) have been developed and investigated for an improved Lithium battery technology. There is no fixed chemistry for the lithium ion cell (unlike the Lead-Acid, Nickel Metal Hydride or Nickel Cadmium batteries), but depends on the unique combination of the anode, cathode and the electrolyte, it gives better performance [1].

In recent years all solid state batteries attained its prime importance due to its application potential towards HEVs and all other high energy density battery requirements. But the development of all solid state battery is in its infancy. The major problem is the development of a sound solid electrolyte. In this scenario, $Li_{0.5}La_{0.5}TiO_3$ (LLTO) is a better candidate due to its very high conductivity at room temperature in the order of 10^{-3} Scm^{-1}. The $LiFePO_4/C$ (LFP/C) is a commercially well identified cathode material, that seeks its application in Lithium metal and Lithium ion battery assemblies. The preparation and properties of LFP/C and LLTO materials at room temperature and its properties at the elevated temperatures has been reported elsewhere [2-4]. The major problem associated with LLTO is related with its interface to the cathode and the anode counter parts. The lack of scientific knowledge towards the interface problems further worsens the situation. The Cyclic Voltammetry (CV) is a powerful tool to analyze the interface properties by analyzing the reversible nature of the sample in details. The study gives a better insight towards the reversibility of the Li-ions with the chosen electrode-electrolyte system. The cycling behavior of the system accompanies oxidation and reduction reactions which appear as respective peaks in the CV pattern [5-9].

The present study addresses the LFP/C cathode, LLTO electrolyte interface for its reversible electrochemistry, when it is assembled in all solid state configurations. The prepared cathode, electrolyte and the thin film battery assembly has been electrochemically characterized by the Cyclic Voltammetric studies using the electrochemical workstation (BIO-LOGIC SP-150). The major concern of the present study is the verification of the electrochemical reversibility of the individual cathode (LFP/C), the electrolyte (LLTO) and its interface.

2. PREPARATION AND CHARACTERIZATION

The $Li_{0.5}La_{0.5}TiO_3$ and $LiFePO_4/C$ has been prepared by sol-gel method. The preparation of LLTO nano-particles at a calcination temperature of 900ºC and nano LFP/C material at 700ºC has been reported elsewhere [2-4]. The composite electrodes consists of 1) Active materials 85 wt%; 2) High surface area Carbon 5 wt%; 3) and the Polymer binder 10 wt%. Copper/Aluminium current collectors are used as the substrate for the electrodes and for the thin film battery assembly. The LFP-C (85%), Carbon Black (5%) and PVdF (10%) were ground together using N-Methyl Pyrrolidione (NMP) to form good slurry. The slurry has been applied to the current collector using the doctor blade apparatus to form a uniform thickness of 10µm. The coated composite has been dried in a controlled atmosphere for about 24 hrs for the cathode preparation.

The LLTO (90%) and PVdF (10%) were ground together using N-Methyl Pyrrolidoine (NMP) to form good slurry. The Slurry has been applied to the current collector using the doctor blade apparatus in to a uniform thickness of 10µm. The coated composite has been dried in a controlled atmosphere for about 24 hrs.

The solid state thin film batteries have been prepared to analyze the electrochemical cycling behavior of the sample. The LFP-C cathode slurry has been coated by doctor blade method on the Copper current collectors as explained above. It has been dried in a controlled atmosphere for 24 hrs. The LLTO inorganic solid electrolyte slurry has been applied about 50% of the total surface of the substrate, above the cathode layer. After proper drying, a layer of anode coating has been carried out about 50% of the LLTO coated area. The anode has been chosen as the slurry of Carbon black (85%) and PVdF (15%), Indium (85%) and PVdF (15%), Lithium Titanate (Li_2TiO_3) (85%) and PVdF (15%), in three different configurations. The prepared assembly has been dried properly before the electrochemical characterization.

3. RESULTS AND DISCUSSION

3.1. Electrochemical Analysis of LFP-C with LFP-C|$LiNO_3$|Pt Configuration

The LFP-C is tested with different electrochemical system to analyze the redox activity and the corresponding changes in the redox behavior with respect to the counter

electrode material. The electrochemical experiments were carried out by designing a conventional type aqueous three-electrode glass cell suffused in aqueous electrolyte. Cyclic Voltammetry has been employed to study the electrochemical activity of electrodes during intercalation and deintercalation reaction with different scan rates. The LFP-C positive electrode with an active area of $1cm^2$, Carbon (C)/Indium (In)/Platinum (Pt) metal strip and the Ag/AgCl were used as the working, counter and reference electrodes, respectively. The aqueous saturated $LiNO_3$ solution was used as the electrolyte. The prepared cathode materials have been analyzed in different configuration with different counter electrodes as follows, in which LFP-C|$LiNO_3$|Pt gives better electrochemical performance.

In this configuration (LFP-C|$LiNO_3$|Pt), unlike A (LFP-C|$LiNO_3$|C) and B (LFP-C|$LiNO_3$|In), prominent redox peaks has been obtained which can be assigned to the redox activity of Fe ions in the LFP-C with reference to the Ag/AgCl electrode. The Fig. 1(a) shows the CV plot of the sample at different scan speeds from 30 mV/sec to 100mV/sec. The first cycle with slow scan speed of 10 mV/sec in Fig. 1(b) exhibit one more oxidation peak nearly at -0.027 V, which can be assigned to the electrolyte contribution in this configuration, which is less prominent at higher scan rate.

All the plots exhibit its characteristic oxidation peak around 0.201V and reduction peak around -0.17V with $LiNO_3$ liquid electrolyte. This is in tune with the result obtained by Sauvage et al. [10] with the LFP-C/$LiNO_3$/Pt configuration using the Saturated Calomel Electrode (SCE) as the reference electrode. The average voltage difference between oxidation and reduction peak is found to be 380 mV. The oxidation and reduction peak positions are observed to be slightly shifted at lower scan rates so that the potential difference between oxidation and reduction is slightly reduced. The intercalation/de-intercalation peak current is linearly related to the root of scan rate Fig. 1(f), establishing the reversible nature of the prepared electrodes. From the Fig. 1(f), oxidation peak current shows a slight variation at lower scan speed, which can be considered as the changes during the stabilization of the material during the initial cycles. In the present case, the peak potential is independent of the scan rate which also confirms the reversible nature of the system. That is the peak potentials are not varying with increasing or decreasing the scan rate which is shown in the CV plot.

For a perfect reversible system, the anodic and cathodic peak currents should have the same magnitude [11]. However, Fig. 1(a) shows that this is not the case for the present LFP, i.e., i_c/i_anot equal to 1. This is because in LFP, the Li ion undergoes a two-phase process during charge and discharge, Li ions are most likely transported through regions with $FePO_4$ or LFP [12,13]. This difference in electrochemical environments [14] for Li movement may account for the difference in the magnitude of the peak current.

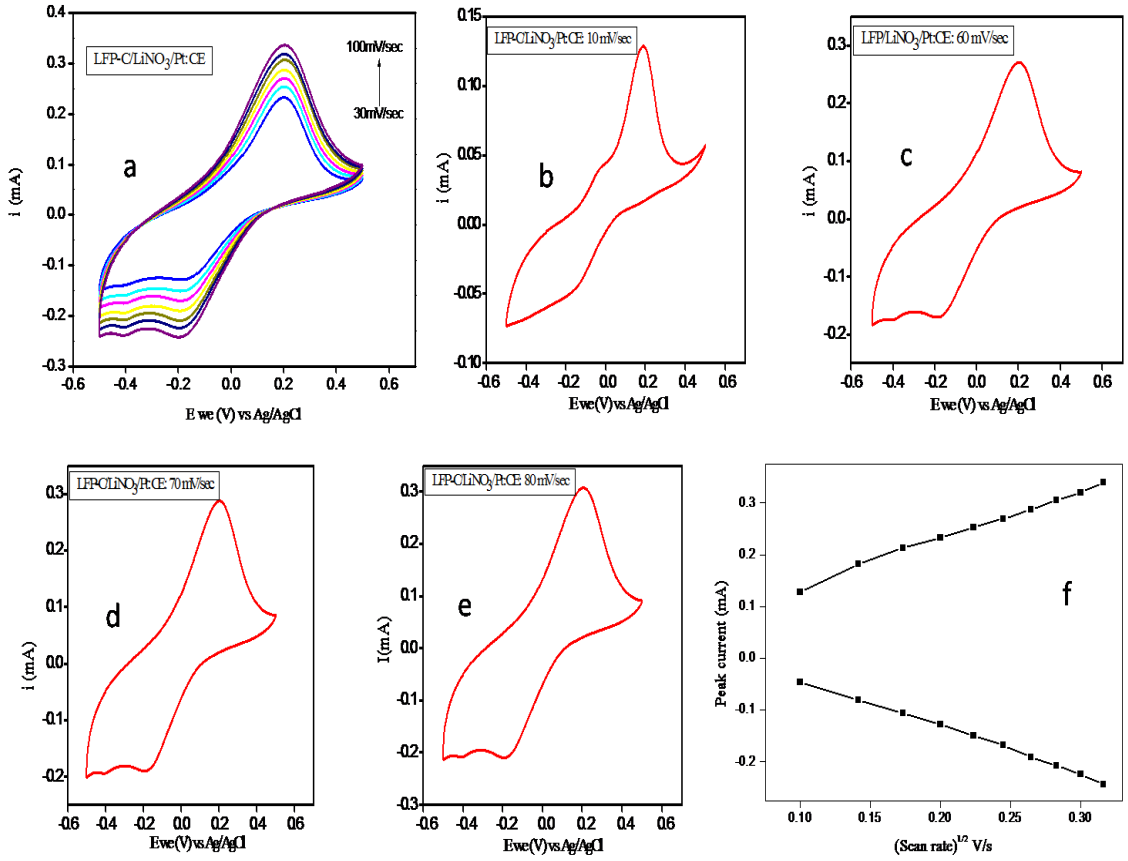

Fig. 1 (a) The CV plot for LFP-C|$LiNO_3$|Pt for different scan speeds **(b)** The CV plot for LFP-C|$LiNO_3$|Pt for the scan speed of 10 mV/sec, **(c)** The CV plot for LFP-C|$LiNO_3$|Pt for the scan speed of 60 mV/sec, **(d)** The CV plot for LFP-C|$LiNO_3$|Pt for the scan speed of 70 mV/sec **(e)** The CV plot for LFP-C|$LiNO_3$|Pt for the scan speed of 80 mV/secm, **(f)** The Peak current versus square root of scan rate for LFP-C|$LiNO_3$|Pt configuration.

In actual experiments, CV profiles are rarely ideal because of the kinetic limitations such as solution resistance and solid-state reactions. In particular, systems involving Li intercalation are more complicated than solution-based systems because the electrode material itself undergoes reaction with transport of Li ions into and out of the electrode and the active material. The CV parameters and observations have been tabulated in Table 1.

3.1.1. Diffusion Co-efficient

The peak current is related to diffusion coefficient by the relation [15]:

$$i_p = 0.446F(F/RT)^{1/2} C^* \nu^{1/2} AD^{1/2} \quad (1)$$

where, i_p is the peak current in Amp, F is the Faraday constant, C* is the initial concentration in mol/cm^3, v is the scan rate in V/s, A is the electrode area in cm^2, D is the diffusion coefficient in cm^2/s, R is ideal gas constant and T is the temperature. The diffusion coefficient indicates the Li ions diffusibility into the electrode material.

Table 1. The CV parameters for the LFP-C|$LiNO_3$|Pt configuration

Samples	Scan Rate (mV/sec)	Peak Potential (V)		Potential Difference (V)	Peak Current Ratio	Diffusion Coefficient (cm^2s^{-1})	
		V_o	$-V_R$			Anodic (x 10^{-7})	Cathodic (x 10^{-7})
LFP-C/$LiNO_3$/Pt	**30**	0.2015	0.1703	0.3718	0.50	2.01	1.00
	40	0.2044	0.1611	0.3759	0.59	1.90	1.00
	50	0.2015	0.1703	0.3765	0.62	1.85	1.10
	60	0.2015	0.1744	0.3811	0.66	1.80	1.10
	70	0.2021	0.1744	0.3821	0.68	1.77	1.20
	80	0.2015	0.1796	0.384	0.70	1.76	1.20
	90	0.2015	0.1773	0.3874	0.74	1.74	1.20
	100	0.2044	0.1796	0.388	0.76	1.75	1.30

The Li ion diffusion in LFP-C is associated with electron transport phenomena due to the Fe reduction/oxidation. The gradient in chemical composition largely affects the transport process in LFP-C mixed conducting electrodes. The higher value of diffusion co-efficient also shows an effective Li ion diffusion in the prepared LFP-C. The stable structure and the homogeneous Carbon encapsulated morphology of the prepared LFP-C electrode leads to the higher diffusion coefficient of the sample.

With Indium or Carbon electrodes the oxidation peak could not be observed within the range of the potential that has been analyzed. The reduction peak obtained also found to be faded to a larger extent. This may be due to the reactivity of Carbon with the active material, which gives multi-phase reduction [14] in the presence of liquid electrolyte. But in the case of Pt electrode since it is non-reactive it exhibits well resolved intercalation/de-intercalation peaks in the liquid electrolyte configuration. From the electrochemical

analysis of the LFP-C electrode with different counter electrodes, it is clearly observed that the counter electrode plays a major role in the electrochemical reversibility of the LFP-C system.

3.2. Electrochemical Analysis of LLTO|$LiNO_3$|Pt

In the chosen configuration, current flow occurs between the LLTO and Platinum with the reference electrode Ag/AgCl, which has been analyzed over the range of voltage -1V to +1V. The Cyclic Voltammetry (CV) is analyzed for different scan rates varying from 30 mV/sec to 100 mV/sec. The Fig. 2(A) shows the CV plots of LLTO for different scan speed of 30 mV/sec to 100 mV/sec. A well resolved oxidation peak and a faded reduction peak, has been obtained with an average peak separation of 598 mV. Redox peaks are observed corresponding to the oxidation/reduction potentials of the redox reactions of Ti^{2+}/Ti in the LLTO sample [16]. Here, broader reduction peaks indicate higher electrode kinetics at the cathode-electrolyte interface during the de-intercalation of the Li^+ ions [17].

In order to verify the nature of the oxidation and reduction peaks after multiple cycles, the LLTO has been tested at a scan rate of 200 mV for 25 cycles (Fig.2 (b)). Even after 25 cycles much capacity fading could not be observed in the present sample. Also the Li^+ intercalation/de-intercalation occurs with negligible volume change, indicating high stability of the prepared LLTO material [18]. The CV plots for 60 mV/sec, 70 mV/sec and 80 mV/sec are shown in Fig.2 (c, d, e) clearly exhibits there is no capacity fading and/or the change in the symmetry of the redox peak at higher scan speeds. Hence it can be concluded that on cycling, not much capacity fading was observed.

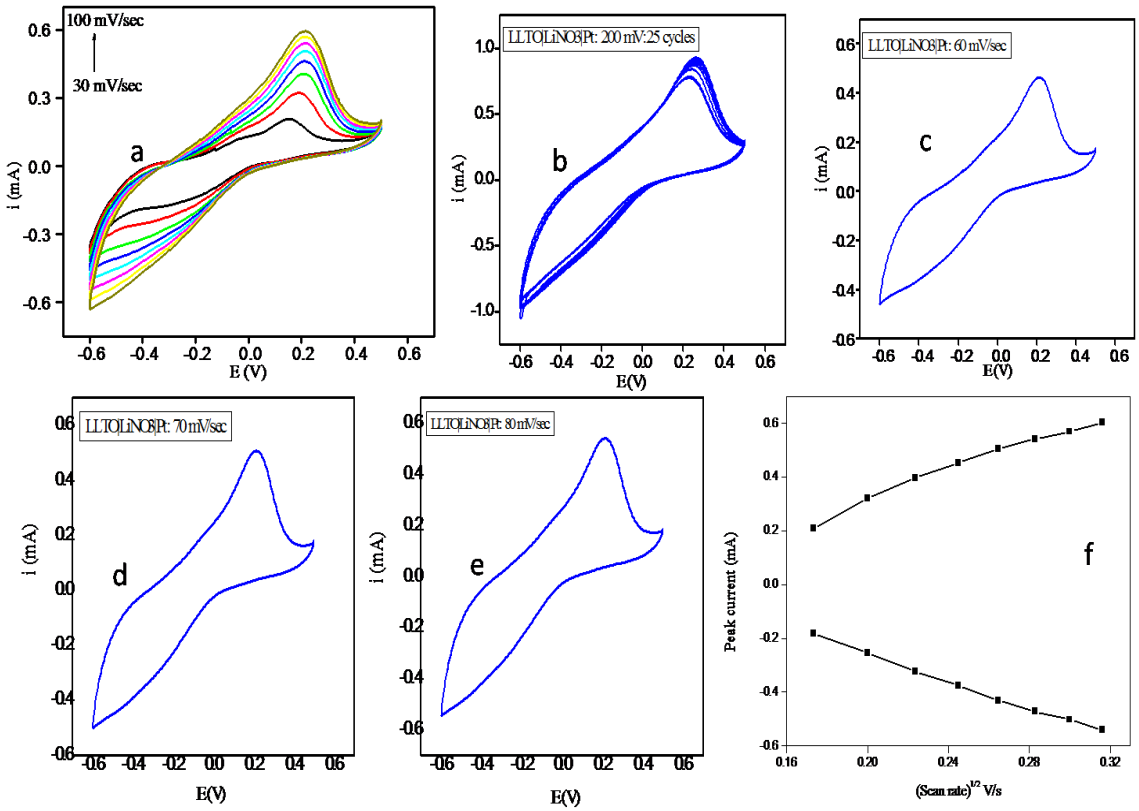

Fig. 2 (a) The CV plot for LLTO|$LiNO_3$|Pt for different scan speed, **(b)** The CV plot for LLTO|$LiNO_3$|Pt for multiple cycles (25 cycles), **(c)** The CV plot for LLTO|$LiNO_3$|Pt for the scan speed of 60 mV/sec, **(d)** The CV plot for LLTO|$LiNO_3$|Pt for the scan speed of 70 mV/sec, **(e)** The CV plot for LLTO|$LiNO_3$|Pt for the scan speed of 80 mV/sec, **(f)** The Peak current Vs square root of scan rate LLTO|$LiNO_3$|Pt.

Table 2. The CV Parameters for the LLTO|$LiNO_3$|Pt Configuration

Samples	Scan Rate (mV/sec)	Peak Potential (V)		Potential Difference (V)	Peak Current Ratio	Diffusion Coefficient (cm^2s^{-1})	
		V_a	$-V_c$			Anodic ($\times 10^{-7}$)	Cathodic ($\times 10^{-7}$)
LLTO	30	0.150	-0.344	0.4932	-0.866	2.59	2.20
	40	0.190	-0.393	0.5934	-0.68266	3.45	2.70
	50	0.203	-0.412	0.6044	-0.68541	3.83	3.10
	60	0.210	-0.431	0.6132	-0.65125	3.98	3.30
	70	0.213	-0.456	0.6152	-0.64744	4.11	3.50
	80	0.2136	-0.464	0.6205	-0.6519	4.05	3.60
	90	0.216	-0.462	0.6246	-0.64649	3.99	3.50
	100	0.211	-0.469	0.6274	-0.65627	3.97	3.50

The Fig. 2 (f) shows the peak current Vs root of scan rate for different cycles of LLTO. The peak current linearly increases with the square root of scan rate which clearly establishes the reversibility of the sample. The peak current ratio also suggests the quasi reversibility of the sample under the present configuration. The CV parameters have been tabulated in table 2. The higher value of diffusion coefficient shows an easier diffusion of the Li^+ ions across the lattice containing stable perovskite structure [18]. The diffusion at Lithium intercalation cycle is much faster when compared to the de-intercalation cycle.

3.3. Electrochemical Analysis of the Battery Configuration

The electrochemical reversibility has also been attempted for different thin film battery configuration to analyze the interface with respect to different anodes in solid state battery configuration. The battery has been fabricated in the following different configurations: LFP-C|LLTO|C (A), LFP-C|LLTO|In (B), LFP-C|LLTO|LTO (C)

The LFP-C|LLTO|C thin film battery system has been tested for its cyclability and oxidation-reduction property at the interface of the fabrication. The Fig.3 (a) shows the CV plot of the battery assembly at the scan rates of 1 mV/s with Carbon anode. The battery assembly exhibits cyclability over a range of voltage from 0 to 1.6V, across the solid state LLTO electrolyte in thin film battery configuration. The assembly sweeps for multiple cycling but the chemical kinetics could not be observed due to either insufficient active material or non-reactivity. The option of non-reactivity is ruled out as the components LFP-C and LLTO exhibited cyclability in aqueous cells. Hence, the insufficient activity or chemical potential difference may be the major reason for non-reactivity. The Fig. 3 (b) shows the first 25 cycles of this configuration at the scan speed of 200 mV/sec. This clearly shows the repeatability of this configuration even at high scan speed over multiple cycles. Here the CV plot suggests an electronic charge transfer instead of ionic mass transfer.

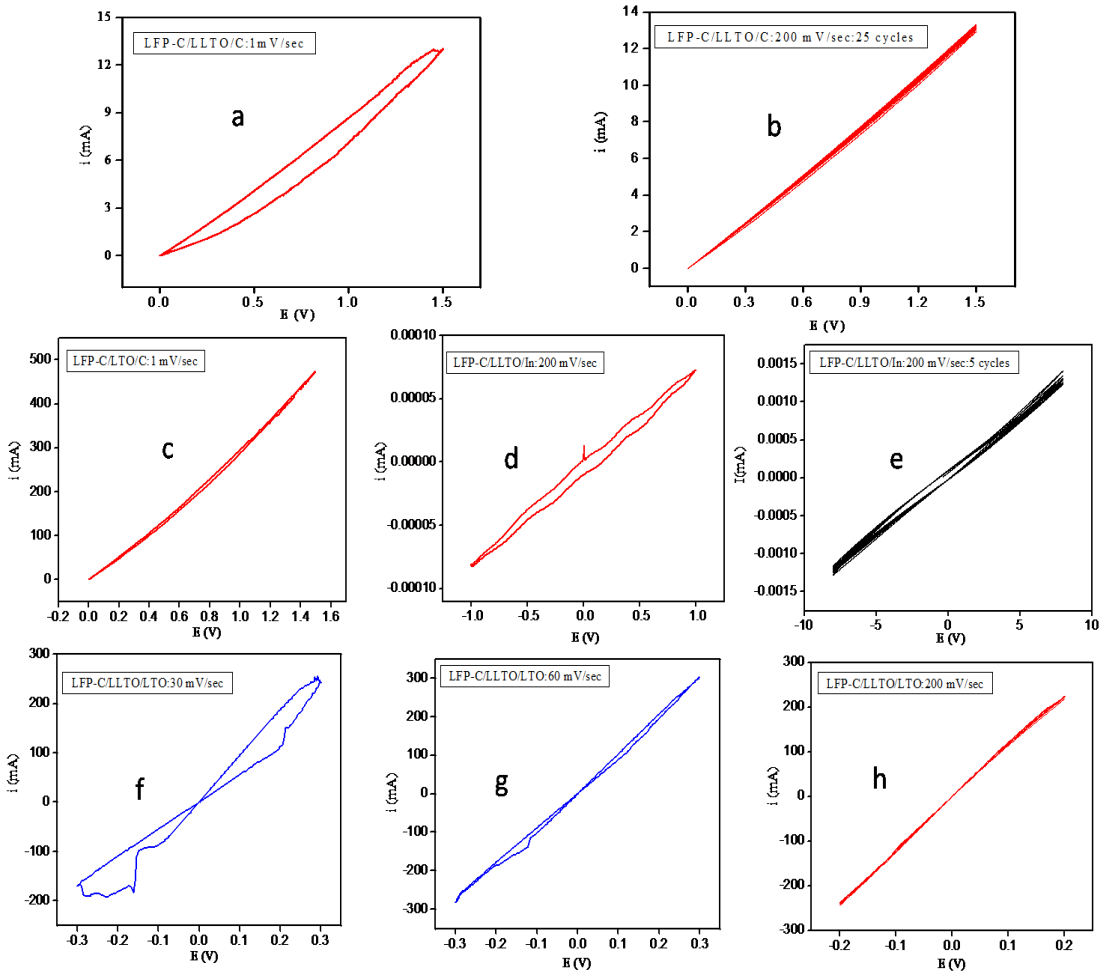

Fig. 3 (a) The CV plot for LFP-C|LLTO|C for the scan speed of 1 mV/s, **(b)** The CV plot for LFP-C|LLTO|C for multiple cycles [scan speed of 200 mV/sec], **(c)** The CV plot for LFP-C|LLTO|In for the scan speed of 1 mV/sec, **(d)** The CV plot for LFP-C|LLTO|In for the scan speed of 200 mV/sec, **(e)** The CV plot for LFP-C|LLTO|In for multiple cycles ata scan speed of 200 mV/sec, **(f)** The CV plot for LFP-C|LLTO|LTO for the scan speed of 30 mV/sec, **(g)** The CV plot for LFP-C|LLTO|LTO for the scan speed of 60 mV/sec, **(h)** The CV plot for LFP- C|LLTO|LTO for multiple cycles at a scan speed of 200 mV/sec.

The Fig. 3 (c) shows the CV plot of LFP-C|LLTO|In thin film assembly at the scan speed of 1mV/s. Similar to LFP-C|LLTO|C system, when Indium metal has been used as the anode, multiple cycles with the absence of redox peaks has been obtained due to the same reasons as explained for Carbon. However, in this configuration, when the scan rate increased beyond 100 mV/sec, a remarkable behavior like Coulomb blockade that occurs in 1D electronic conductor especially in nano-dimensions ensuring the existence of electronic charge transfer has been observed. It shows 1D type symmetric movements of the electrons/ions extending to the exact voltage range of +1V to -1V. Here, since the LLTO solid electrolyte has the property that it can very easily reduce to Ti^{3+} ions with the

release of electrons so that there is a better chance for this to develop as an electronic conductor in contact with some anodes. Since, the LLTO and LFP-C is in the nano-dimension this type of mechanism which occurs in double tunnel devices can be expected. Such coulomb stair cases can occur for a conductor sandwiched between two insulators. Hence, it is clear that double layers developed on the anode/electrolyte and cathode/electrolyte interfaces acts as insulators with LLTO as a conductor. Thus resulting 1D like behavior. The origin and the effect of this property has to be analyzed separately which is out of the scope of this article.

The LFP-C/LLTO interface has also been assembled with LTO anode material, in thin film battery configuration. The Fig. 3 (f) shows the CV plot of LFP-C|LLTO|LTO assembly at a scan speed of 30 mV/sec, whose behavior is extremely different. The onward potential step and backward potential sweeps resulting to different resistances across the sandwich indicating that the insulating interfaces produced on either side of LLTO have different resistances. Again this assembly has not allow Li^+ to intercalate/deintercalate which remains as a challenge. Thus it is systematically made clear that both the interfacial surfaces alters the trend of operation of an electrochemical cell and all solid state battery still have an interfacial problem to be severely addressed with for furtherance [15]. In order to analyze the interaction between LLTO solid electrolyte and the LFP-C cathode material, whether it forms some non-passivating layers or makes irreversible changes during the assembly, the LLTO:LFP-C mixed sample is also analyzed with the liquid electrolyte ($LiNO_3$) with Ag/AgCl reference electrode and Platinum counter electrode system.

3.4. Electrochemical Analysis of the LLTO: LFP-C Mixed Sample

The Fig. 4 (a) show the CV plot of the LLTO/LFP-C mixed sample over a scan speed of 30 mV/s to 100 mV/s. Well resolved redox peaks corresponding to the LFP-C and LLTO has been observed in the CV plot of the mixed sample. The mixed sample exhibits three oxidation peaks two well resolved reduction peaks within the voltage range of the present investigation. The oxidation peaks are obtained around 0.21, -0.12V and -0.34V. The LFP-C|$LiNO_3$|Pt configuration exhibits the oxidation peak at 0.20V, the LLTO|$LiNO_3$|Pt, also exhibits its characteristic oxidation peak at 0.21V with a reference electrode Ag/AgCl. The mixed sample exhibits an extended peak in this region from

0.06V to 0.28V. The oxidation peaks at -0.12V and -0.34V, are associated with the dissociation of water and electrolyte respectively [19].

The mixed sample exhibits two reduction peaks at -0.173V and -0.39V. The LFP-C|$LiNO_3$|Pt configuration exhibits a reduction peak at -0.17V, and the LLTO|$LiNO_3$|Pt exhibits its characteristic reduction peak at -0.40V with the Ag/AgCl reference electrode. Hence, the first reduction peak can be assigned to the LFP-C due to the Fe ion reduction and the second peak can be assigned to LLTO due to the reduction of Ti ions during the deintercalation of the Li^+ ions.

The Fig. 4(b) shows the CV plots of the mixed sample over 25 cycles with a scan speed of 200 mV/sec. The Fig. 4(c, d, e) shows the CV plots of the mixed sample at different scan speed of 60 mV/sec, 70mV/sec, 80mV/sec respectively. The figure shows a homogeneous symmetric repetition of cycles without any fading. Hence from the CV characterization of the LLTO:LFP-C mixed sample, it is evident that eventhough the fading due to high interfacial resistance [9] observed in the CV plot, the LLTO/LFP-C interface exhibits reversible electrochemistry over multiple cycles without fading.

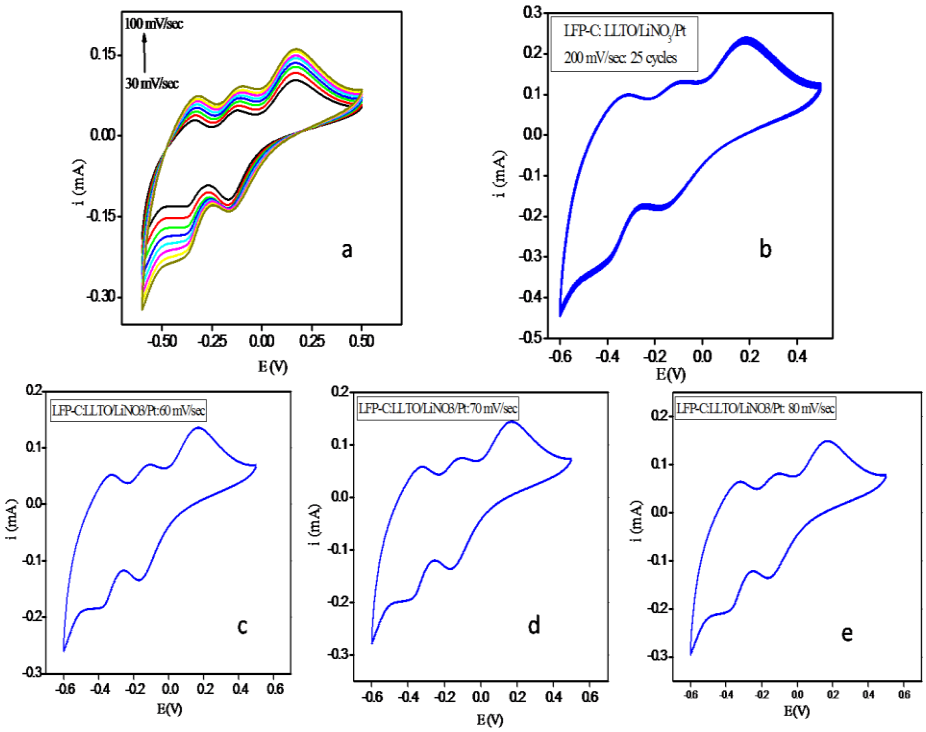

Fig.4 (a) The CV plot for LFP-C:LLTO/$LiNO_3$/Pt for different scan speed of 30 mV/sec to 100 mV/sec, **(b)** The CV plot for LFP-C:LLTO/$LiNO_3$/Pt for the scan speed of 60 mV/sec, **(c)** The CV plot for LFP-C:LLTO/$LiNO_3$/Pt for the scan speed of 70 mV/sec,

(d) The CV plot for LFP-C:LLTO/$LiNO_3$/Pt for scan speed of 80 mV/sec, **(e)** The CV plot for LFP-C: LLTO/$LiNO_3$/Pt for scan speed of 200 mV/sec for 25 cycles.

4. CONCLUSION

The prepared LFP-C, LLTO materials have been analyzed for their electrochemical reversibility with liquid electrolyte ($LiNO_3$) using Carbon, Indium and Platinum anodes and Ag/AgCl reference electrodes. With Carbon and Indium anodes the LFP-C did not exhibit any oxidation peak. The LFP-C and LLTO shows well resolved redox peaks with Pt contact electrodes in liquid electrolyte configurations. The assembled thin film battery also shows severe capacity fading even with slower scan rate. With the LTO anode, the assembled thin film battery shows more electronic behavior. There is a slight change in the reduction peak potential of the LLTO solid electrolyte in the mixed sample, which can be attributed to the interfacial effects of the sample across the LLTO/LFP-C. But the LLTO, LFP-C and mixed samples give the redox peaks independently with the liquid electrolyte configuration. Hence, the severe reactivity with the LFP-C and LLTO electrolyte has been ruled out in the present attempt. The development of high resistance across the interface after cycling might have some important impact across the interface region. But from the analysis of the mixed sample, it has been inferred that even this resistance did not create any nonreversible changes in the CV plots. Hence, it is concluded that the sandwich between LLTO/LFP-C is a right choice in proceeding towards all solid state battery, while the identification of a better anode in its potential window creates the additional challenges.

REFERENCES

[1] MV Reddy, GV Subba Rao, BVR Chowdari, Metal oxides and oxy-salts as anode materials for Li ion batteries , Materials Review, 113(7) (2013) 5364-5457.

[2] Hsu, K.F.; Tsay, S.Y.; Hwang, B.J. Synthesis and characterization of nano-sized $LiFePO_4$ cathode materials prepared by a citric acid-based sol-gel route. Journal of Materials Chemistry, 14 (2004) 2690–2695.

[3] K.P. Abhilash, P.Sivaraj, P.Christopher Selvin, B.Nalini, K.Somasundaram, Investigation on spin coated LLTO thin film nano-electrolytes for rechargeable lithium ion batteries" Ceramics International, 41 (2015) 13823–13829

[4] K.P. Abhilash, P.Christopher Selvin, B.Nalini, K.Somasundaram, P. Sivaraj, A.Chandra Bose, Study of the temperature dependent transport properties in nanocrystalline Lithium

Lanthanum Titanate for Lithium Ion Batteries, Journal of Physics and Chemistry of Solids, 91(2016)114–121.

[5] P.T.Kissinger, W.R.Heineman, "Monographs in Electroanalytical Chemistry and Electrochemistry", Marcel Dekker, New York, (1984) 51.

[6] P.T.Kissinger, W.R.Heineman, Journal of Chemical Education, 60 (1983) 702.

[7] Douglas A.Skoog, F. James Holler, Stanley R.Crouch, "Principles of Instrumental Analysis", Thomson Brookes/Cole, (2007).

[8] Carriedo, Gabino, Journal of Chemical Education, 65 (1988) 65.

[9] Kyosuke Kishida, Naoyuki Wada, Yuji Yamaguchi, Haruyuki Inui, Journal of Materials Research, 25 (2010).

[10] F.Sauvage, E.Baudrin, M.Morcrette, J.M.Tarascon, Electrochemical and Solid State Letters, 7 (2004) A15.

[11] K. Gosser Jr., "Cyclic Voltammetry", VCH Publishers, INC., New York, (1994).

[12] A. K. Padhi, K. S. Nanjundaswamy, J. B. Goodenough, Journal of the Electrochemical Society, 144(1997)1188**.**

[13] V. Srinivasan, J. Newman, Journal of Electrochemical Society, 151 (2004) A1517.

[14] P.Rosaiah, P.Jeevan Kumar, K.JayanthBabu, O.M.Hussain, Applied Physics A, 113 (2013) 603-611.

[15] A.J.Bard, L.R. Faulkner, Electrochemical Methods, John Wiley and Sons, Inc., New York (1980).

[16] K.Vijayababu, V.Veeraiah, P.S.V.Subba Rao, International Journal of Scientific and Engineering Research, 3 (2012)1.

[17] Denis Y.W.Yu, Christopher Fietzek, Wolfgang Weydanz, Kazunori Donoue, Takao Inoue, Hiroshi Kurokawa, Fujitani, Journal of the Electrochemical Society, 154 (2007) A253.

[18] YujingSha, Tao Yuan, BoteZhao,RuiCai, Huanting Wang, Zongping Shao, Journal of Power Sources, 231 (2013) 177.

[19] Can Cao, Zhou Bin Li, Xian-Liang Wang, Xin-Bing Zhao, Wei-Quang Han, Frontiers Energy Research, 2 (2014) 1.